

Determination of Critical State Parameters in Sandy Soils from Standard Triaxial Testing (II) : Experiment and Recommendation

표준삼축시험으로부터 사질토에서의 한계상태정수 결정에 관한 연구 (II) : 실험 및 추천

Cho, Gye-Chun*

조 계 춘

요 지

사질토에서의 한계상태정수 결정시 근본적인 물리적 과정들과 고유적인 한계성들을 파악하기 위하여 일련의 표준삼축시험을 실시하였다. 시험결과에 의하면, 주어진 흙에 대하여 한계상태마찰각은 배수조건에 상관없이 일정한 반면에, e - $\log p'$ 공간상에서의 한계상태선은 주로 표준삼축시험에서 충분치 못하게 도달하는 변형률과 비배수시험에서의 변형률 국지화효과 때문에 배수조건에 따라 다른 결과를 보였다. 실내시험을 통하여 한계상태정수를 산정하는 최선의 방법은 균일하고 느슨하게 성형된 시료를 배수조건하에서 전단하는 것으로 나타났다. 더불어 배수시험에서 다일러턴 시효이나 변형률 국지화효과를 피할 수 있는 시험을 계획하기 위한 참고상태정수를 제시하였다.

Abstract

A set of standard triaxial testing was performed to identify underlying physical processes and inherent limitations in the determination of critical state parameters in sandy soils. The experimental test results showed that the critical state friction angle for a given soil is constant regardless of drainage condition while the critical state line on the e - $\log p'$ space is significantly affected by drainage condition mainly because of insufficient strain attained in standard triaxial tests and strain localization effects in undrained tests. It appeared that the best method to determine critical state parameters in laboratory testing is to use homogeneous loose specimens under drained shear condition. In addition, a reference state parameter was suggested to design tests that will avoid dilatancy or strain localization effects in drained tests.

Keywords : Critical state, Critical state parameters, Friction angle, Post-liquefaction, Sandy soil, Strain localization, Shear strength, Standard triaxial test

1. Introduction

Liquefaction is the phenomenon, which can be often found in sandy soils, whereby a soil deposit experiences a drastic reduction in shear strength. The remaining resistance to shear deformation is referred to as the post-liquefaction shear strength (i.e. reliable ultimate

shear strength). Criteria for liquefaction susceptibility are summarized in Table 1.

Liquefaction is related to flow failures, lateral spreading, and level-ground liquefaction. These phenomena fall under two categories: cyclic mobility and flow liquefaction (Table 2). Cyclic mobility produces unacceptable, large permanent deformations not because of

* Member, Assistant Prof., Civil & Environmental Engrg., KAIST, Daejeon, gyechn@kaist.ac.kr

Table 1. Criteria for liquefaction susceptibility

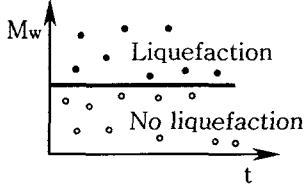
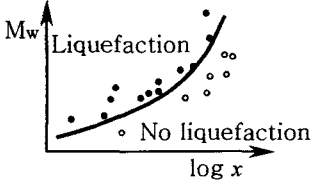
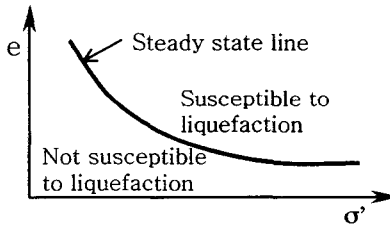
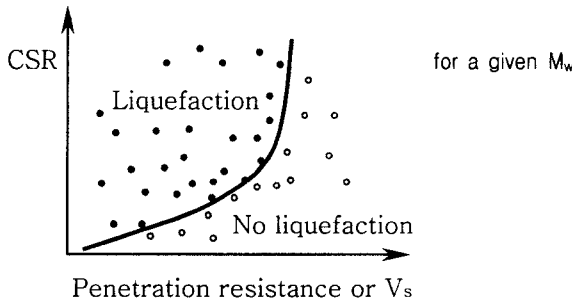
Criteria	Contents		Reference
Historical criterion	<ul style="list-style-type: none"> Moment magnitude (M_w) vs time (t) for a given site. 	<ul style="list-style-type: none"> Moment magnitude (M_w) vs epicentral distance (x). 	Youd (1991), Ambraseys (1988)
Geological criterion	<ul style="list-style-type: none"> Depositional environment: uniform grain size distribution and loose state in fluvial, colluvial and aeolian deposits → high susceptibility to liquefaction. Hydrological environment: liquefaction susceptibility increases with decreasing groundwater depth. Age of a soil deposit: the susceptibility of newer soil deposits to liquefaction is generally higher than that of older deposits (Holocene age > Pleistocene age). 		Youd and Hoose (1977), Kramer (1996)
Compositional criterion	<ul style="list-style-type: none"> Gradation: poorly-graded soils are more susceptible to liquefaction than well-graded soils. Particle shape: rounded-shaped soils are more susceptible to liquefaction than angular-shaped soils. Particle size: the effect of particle size on liquefaction susceptibility is controlled by two competent factors such as compressibility and permeability for a given soil. In general, the criterion of particle size is broad (i.e., fine-grained soils ~ gravels). Liquefaction susceptibility criteria for fine-grained soils Chinese criteria (U.S. Army Corps of Engineers criteria) <ul style="list-style-type: none"> Fraction finer than 0.005mm ≤ 15% (5%) Liquid limit, LL 35% (36%) Natural water content ≥ 0.9 LL (0.92 LL) Liquidity index ≤ 0.75 		Wang (1979), Finn et al. (1994), Kramer (1996)
Steady State criterion	<ul style="list-style-type: none"> Liquefaction susceptibility depends on the initial state such as void ratio and stress. Steady state line can be obtained from laboratory test. 		Castro (1969), Casagrande (1976), Poulos et al. (1985), Been and Jefferies (1985)
Cyclic stress criterion	<ul style="list-style-type: none"> Estimate Cyclic Stress Ratio (CSR) induced by earthquake. Obtain Cyclic Resistance Ratio (CRR) from cyclic triaxial test. Assess susceptibility from safety factor. $CSR = \frac{\tau_{avg}}{\sigma'_v} = 0.65 \cdot \frac{a_{max}}{g} \cdot \frac{\sigma_v}{\sigma'_v} \cdot r_d \quad CRR = \left[\frac{\sigma_{dc}}{2 \cdot \sigma'_v} \right]_{50} \cdot C_r \cdot \frac{D_r}{50}$ $FS = \frac{CRR}{CSR} \quad FS > 1 \rightarrow \text{No liquefaction}$ $FS = \frac{CRR}{CSR} \quad FS \leq 1 \rightarrow \text{Liquefaction}$		Seed and Idriss (1971), Youd and Idriss (1997)
Cyclic strain criterion	<ul style="list-style-type: none"> Determine γ_c and n. Compare γ_c with the threshold strain of the soil. If $\gamma_c < \gamma_t$, no liquefaction will occur. Otherwise, estimate $\Delta u / \sigma'_v$. The value of $\Delta u / \sigma'_v$ estimated is used to decide if the site will experience initial liquefaction ($\Delta u / \sigma'_v = 1.0$) or not. $\gamma_c = 0.65 \cdot \frac{a_{max}}{g} \cdot \frac{\sigma_v \cdot r_d}{G_{max} \cdot (G/G_{max})_c}$		Dobry et al. (1982)

Table 1. (Continued)

Criteria	Contents	Reference
Back analysis criterion	<ul style="list-style-type: none"> Cyclic Stress Ratio (CSR) vs in-situ measurement (SPT, CPT, etc.) 	Seed (1979), Seed, Idriss and Arango (1983), Robertson and Campanella (1985), Youd and Idriss (1997)
Empirical correlation criterion	<ul style="list-style-type: none"> Standard penetration resistance versus earthquake shaking conditions $N_{crit} = N_o [1 + 0.125(D_s - 3) - 0.05(D_w - 2)]$ <ul style="list-style-type: none"> Cone penetration resistance versus earthquake shaking conditions $q_{crit} = q_o [1 - 0.065(D_w - 2)] [1 - 0.05(D_s - 2)]$ <p>Note: N_{crit} and q_{crit} separate liquefiable from nonliquefiable conditions to a depth of 15m.</p>	Chinese building code (1974; from Seed et al., 1983), Zhou (1980)
Probabilistic approach	<ul style="list-style-type: none"> Probability of liquefaction $P_L = [1 + \exp\{- (\beta_0 + \beta_1 \ln(CSR) + \beta_2 (N_1)_{60})\}]^{-1}$ <p>where $(N_1)_{60}$ is the corrected SPT resistance,</p> <p>$\beta_0 = 10.17, \beta_1 = 4.193, \beta_2 = -0.244$ for all sands, $\beta_0 = 16.45, \beta_1 = 6.460, \beta_2 = -0.398$ for clean sand soils, $\beta_0 = 6.483, \beta_1 = 2.685, \beta_2 = -0.182$ for silty sands.</p>	Liao et al. (1988)

Notation:

- e : void ratio
- σ' : effective confining pressure
- τ_{avg} : average shear stress
- n : number of cycles
- σ_v, σ'_v : total and effective overburden pressure
- a_{max} : horizontal maximum acceleration at the ground surface
- g : acceleration of gravity
- σ_{dc} : cyclic deviator stress
- C_r : a correction factor (cyclic – field condition)
- r_d : stress reduction factor
- D_r : field relative density in percent
- G_{max} : shear modulus of the soil at very small cyclic strain ($\sim 10^{-4}\%$)

$$\left[\frac{\sigma_{dc}}{2 \cdot \sigma'_v} \right]_{50} : \text{shear stress ratio causing liquefaction for } D_r = 50\%$$

$(G/G_{max})_{\gamma_c}$: effective modulus reduction factor of the soil corresponding to the cyclic strain, γ_c

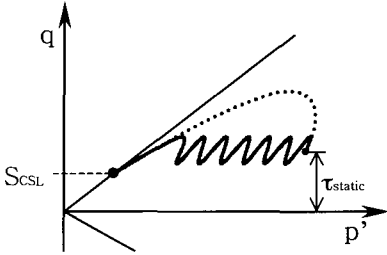
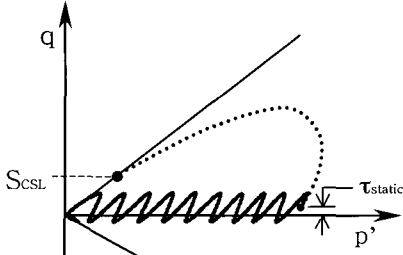
D_s : depth to sand layer under consideration, in meters

D_w : depth of water below ground surface, in meters

N_o & q_o : a function of the shaking intensity as follows

Modified Mercalli Intensity	N_o (blows/ foot)	q_o (MPa)
VII	6	4.6
VIII	10	11.5
XI	16	17.6

Table 2. Comparison of flow liquefaction and cyclic mobility

	Flow Liquefaction	Cyclic Mobility
Behavior		
Initial τ	$\tau_{static} \geq S_{CSL}$	$\tau_{static} < S_{CSL}$
Soil type	Contractive	Low & medium densities
Factors	Not sensitive to initial conditions Depends on σ'_o & e_o Possible effect of loading path May be affected by plastic fines*	Sensitive to - σ'_o & e_o - amplitude excitation - initial stiffness (aging, prestrain, cementation, fabric) - % plastic fines*
Engineering problems	Slope problems (Lateral deformation, flow)	Level ground Early role in slope instability
Uniqueness	Quite unique – easy determination of SS line in $e-p'$ space	Many parameters affect strength due to characteristic of pore water pressure generation
Design approach	Strength is considered	Deformation is considered
Design parameter	$\text{Min}\{[SS \text{ strength}]_{dr}, [SS \text{ strength}]_{und}\}$	Strength @ 5% double-amplitude strain @ 15cycles (5% criterion: good for clean and silty sands)

*Note: % fines may play a more critical role in field performance than in laboratory measurements (t of τ dissipation versus t of earthquake).

SS is steady state.

Notation: S_{CSL} is the critical state shear strength on $p'-q$ space.

insufficient strength but because of the accumulation of shear strain experienced during cyclic earthquake shaking. On the other hand, flow liquefaction produces very large permanent deformation due to insufficient strength reached during monotonic loading, cyclic loading (e.g. earthquakes), and nonseismic vibration sources (e.g. pile driving, train traffic, geophysical exploration, and blasting). Flow liquefaction has been observed in natural and man-made deposits of contractive soils. Examples include the Sheffield Dam failure during the Santa Barbara earthquake in 1925, the Turnagain Heights landslide during the Alaska earthquake in 1964, Kawagishi-cho apartment buildings failure during the Nigata earthquake in 1964, and the Lower San Fernando dam failure during the San Fernando earthquake in 1971.

The post-liquefaction shear strength must be properly determined in order to judge whether or not flow

liquefaction can occur at a site. As suggested as an example in the former paper, the post-liquefaction shear strength can be reliably estimated from the critical state parameters and void ratio. However, the proper methodology for the determination of critical state parameters has not been established. In this paper, underlying physical processes and inherent limitations are identified through experimental tests and a proper procedure is suggested to obtain the critical state parameters from standard triaxial testing.

2. Experimental Setup

A set of conventional triaxial compression tests was performed to identify underlying physical processes and inherent limitations on the determination of critical state parameters in sandy soils.

2.1 Tested Soil – Its Properties

The tested soils include blasting sand, Ottawa 20-30 sand, and sandboil sand. The blasting sand is angular

while the Ottawa 20-30 sand is round. The sandboil sand is a natural soil obtained from a paleoliquefaction site (a site where liquefaction occurred previously) in Arkansas, USA. Relevant information for these materials is sum-

Table 3. Tested soil-Properties

Material	e_{max}	e_{min}	D_{50} (mm)	D_{10} (mm)	C_u	C_c	G_s	R	S	$M(\phi_{cs}^\circ)$	λ	Γ
Blasting sand	1.025	0.698	0.71	0.42	1.94	0.94	2.65	0.30	0.55	1.29 (32)	0.069	1.099
Ottawa 20-30 sand	0.742	0.502	0.72	0.65	1.15	1.02	2.65	0.90	0.90	1.07 (27)	0.047	0.802
Sandboil sand	0.790	0.510	0.36	0.17	2.41	1.29	2.62	0.55	0.70	1.33 (33)	0.051	0.785

Notation: Coefficient of uniformity - $C_u = D_{60}/D_{10}$, Coefficient of curvature - $C_c = D_{30}^2/D_{10} \cdot D_{60}$, Specific gravity - G_s , Roundness - R (mean value), Sphericity - S (mean value), Strength parameter - $M = 6 \sin \phi_{cs} / (3 - \sin \phi_{cs})$, Critical state friction angle - ϕ_{cs} , slope of CSL on $e-\log p'$ - λ , and intercept of CSL at $p' = 1\text{kPa}$ on $e-\log p'$ - Γ .

Note: The maximum void ratio e_{max} is determined by ASTM D4253-93 and the minimum void ratio e_{min} is by ASTM D4254-91.

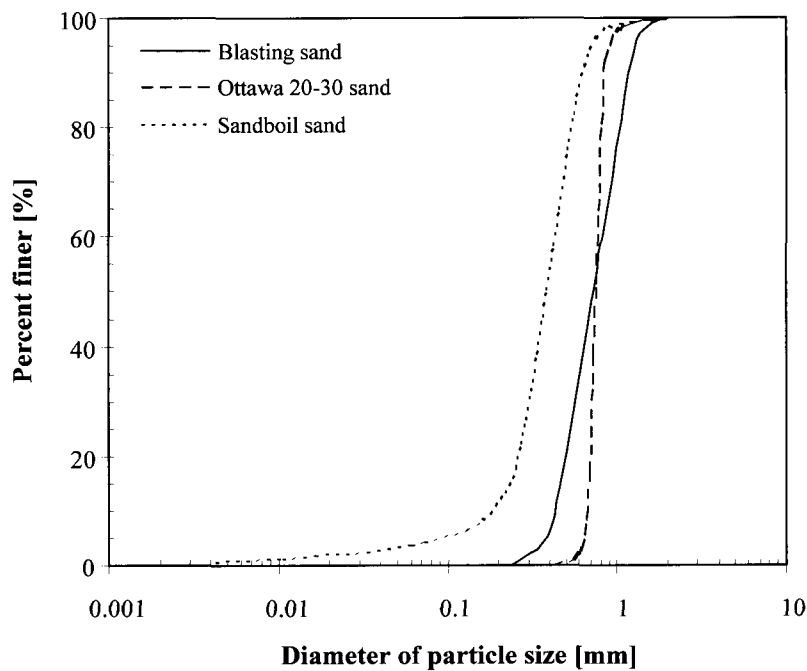
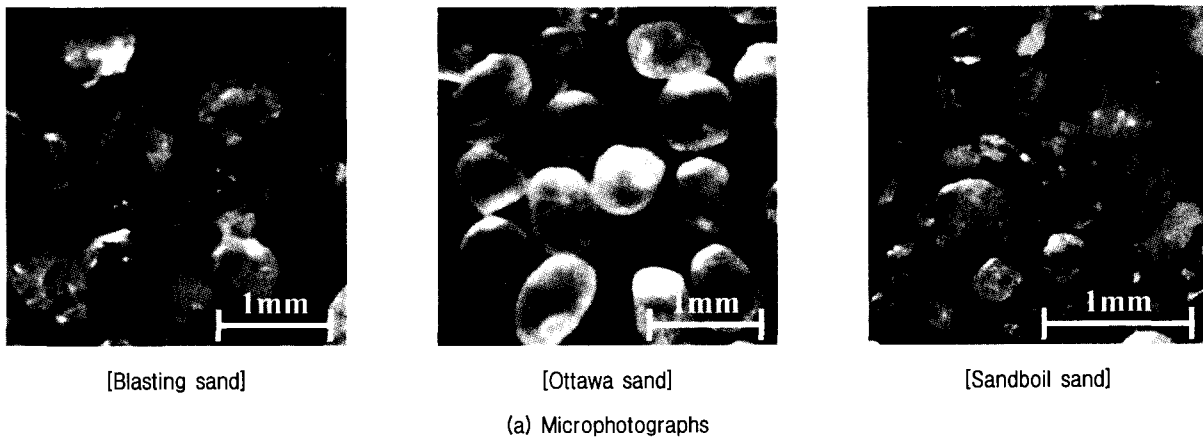


Fig. 1. Microphotographs and particle size distribution for three tested soils

marized in Table 3. Microphotographs and particle size distributions are shown in Fig. 1.

2.2 Preparation and Test Procedures

Specimens have a nominal diameter of 75 mm and height of 150 mm (i.e. a length-to-diameter ratio of 2). A circular aluminum split mold and a 0.033 cm thick latex membrane are used to form and hold the specimen. Full diameter porous stones and a layer of filter paper are placed at the top and bottom plates.

Loose contractive specimens for drained and undrained tests are prepared using the moist tamping procedure. Other sample preparation methods such as air pluviation, water pluviation (for details refer to Park, 2000), and a mixture of soil with salt or ice are attempted to obtain homogeneous loose specimen. However, the moist tamping method is often preferred because of its ability to make specimens loose above maximum void ratio (the spatial variability of specimens made by this method is significant, as discussed in Cho, 2001). Blasting sand and Ottawa 20-30 sand specimens are prepared at 3% water content while 4% water content is used to prepare the sandboil sand. Specimens are compacted in ten layers, scratching and stirring the surface of each layer before placing the next layer to enhance homogeneity.

The specimen is held with a vacuum of 80 kPa before the mold is disassembled. Actual specimen dimensions are carefully measured with calipers to the nearest 0.01 mm, and the initial volume is calculated. After assembling the triaxial cell, the cell is fully filled with water. This allows monitoring volume changes during specimen saturation to accurately evaluate the initial void ratio of the specimen at the time of testing. All specimens are vacuum and back-pressure saturated to ensure that specimens have a high degree of saturation, with Skempton's B values greater than 0.995. Isotropic consolidation is applied in small increments until the selected effective confining stress is reached.

The strain-controlled triaxial tests are performed with a 0.5%/min strain rate for blasting and Ottawa 20-30

sands, and 0.25%/min strain rate for the sandboil sand. These slow strain rates, experimentally determined, promote uniform pore-water pressure within the specimen. Loading continues until 35% axial strain is reached. The automatic data acquisition system records the axial strain, volumetric strain, pore water pressure, and principal stress every 0.01% strain.

End platens are not lubricated in this study since there is little effect of end restraint on the failure stress and volume changes in contractive homogeneous specimens (see Wood, 1990; Hird and Hassona, 1990; Desrues et al., 1996). Membrane stiffness may have an effect on test results when the specimen is subjected to low confining stresses. The additional radial stress contributed by the membrane stiffness is determined by measuring the pressure that must be applied inside the membrane to cause it to expand laterally similar to the final expansion observed during the test. Then, the applied effective confining stress is corrected to exclude the stress contributed by the membrane stiffness.

3. Experimental Results

3.1 Drained Test Results – Localization

Figures 2, 3 and 4 show drained test results for blasting, Ottawa 20-30, and sandboil sand specimens with different initial void ratios at the same effective confining stress. As the initial void ratio decreases, the axial strain at peak stress decreases. The shear stress approaches a similar value in all specimens after ~20% axial strain. However, "globally computed" void ratios do not converge to the same value due to strain localization in the dense specimens, which develop shear bands during testing. The critical state friction angles for blasting sand and sandboil sand (angular particles) are greater than that of Ottawa 20-30 sand (subrounded particles).

Figures 5, 6 and 7 show drained test results for specimens of three sands at similar initial void ratio but with varying effective confining stresses (the initial void ratio decreases with confining stress due to the initial

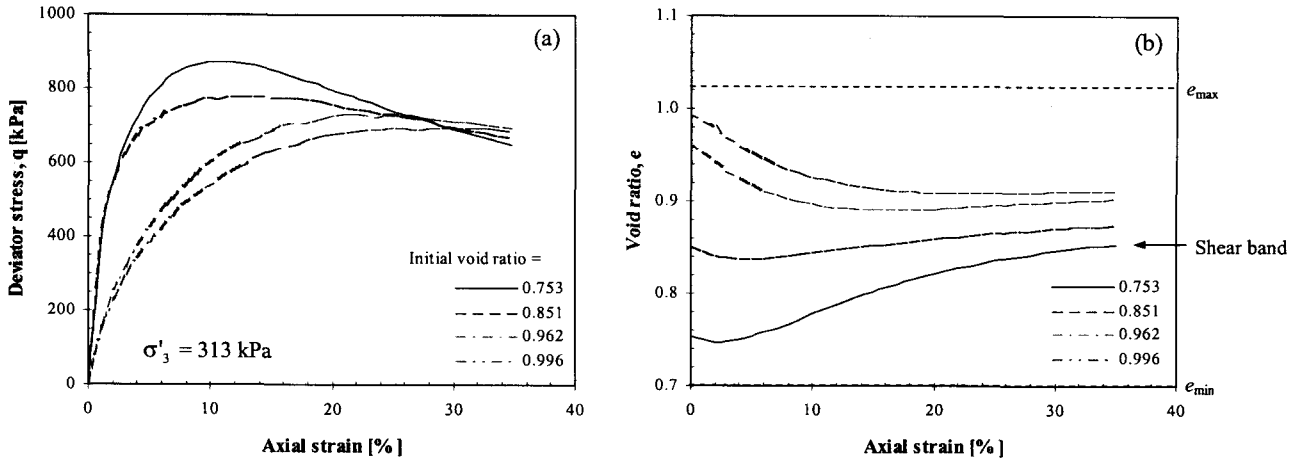


Fig. 2. Drained test results for blasting sand with different initial void ratios at the same effective confining stress ($\sigma'_3 = 313$ kPa)

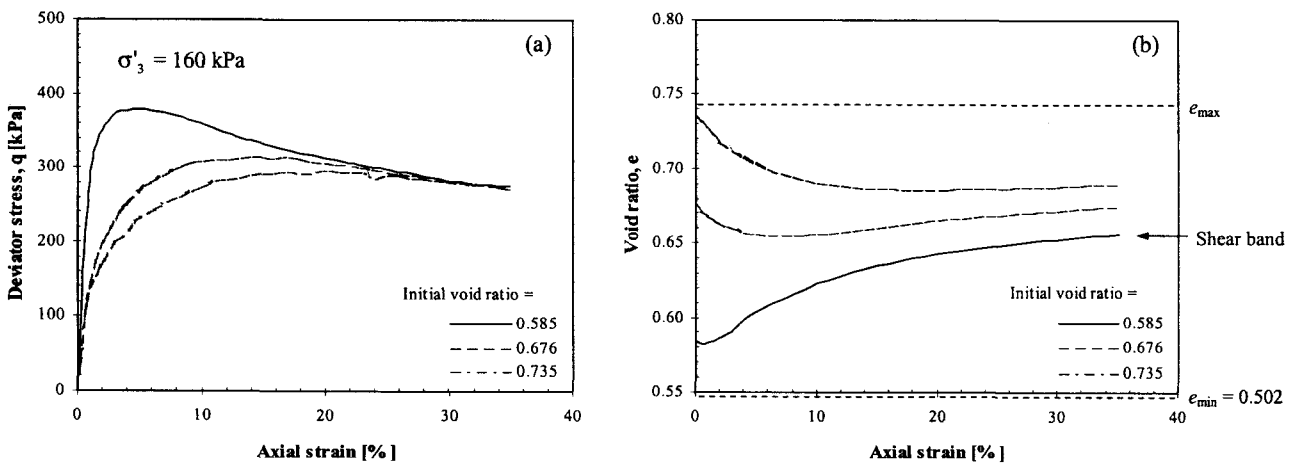


Fig. 3. Drained test results for Ottawa 20-30 sand with different initial void ratios at the same effective confining stress ($\sigma'_3 = 160$ kPa)

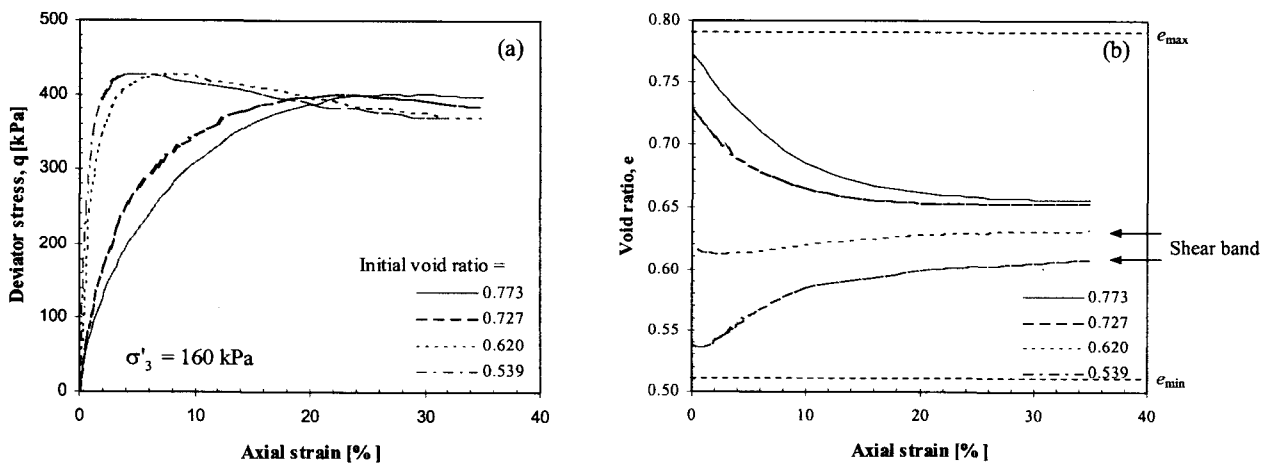


Fig. 4. Drained test results for sandboil sand with different initial void ratios at the same effective confining stress ($\sigma'_3 = 160$ kPa)

consolidation of the specimen). All specimens are prepared in loose homogeneous condition in order to avoid localization effects. All stress-strain responses show decisively contractive behavior and no shear band

formation is observed. Critical state is reached at about 30% axial strain. Critical state parameters f_{cs} , Γ and λ are summarized in Table 3.

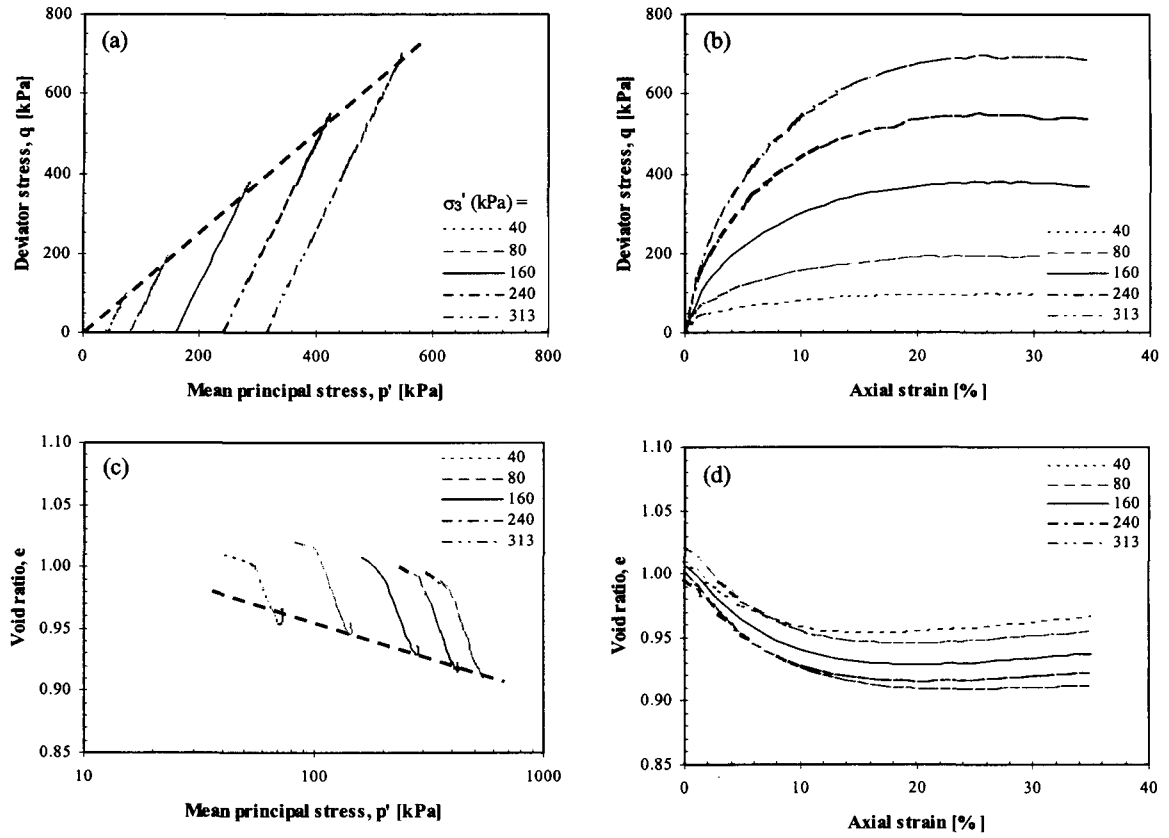


Fig. 5. Drained test results for blasting sand with varying effective confining stresses and similar initial void ratio

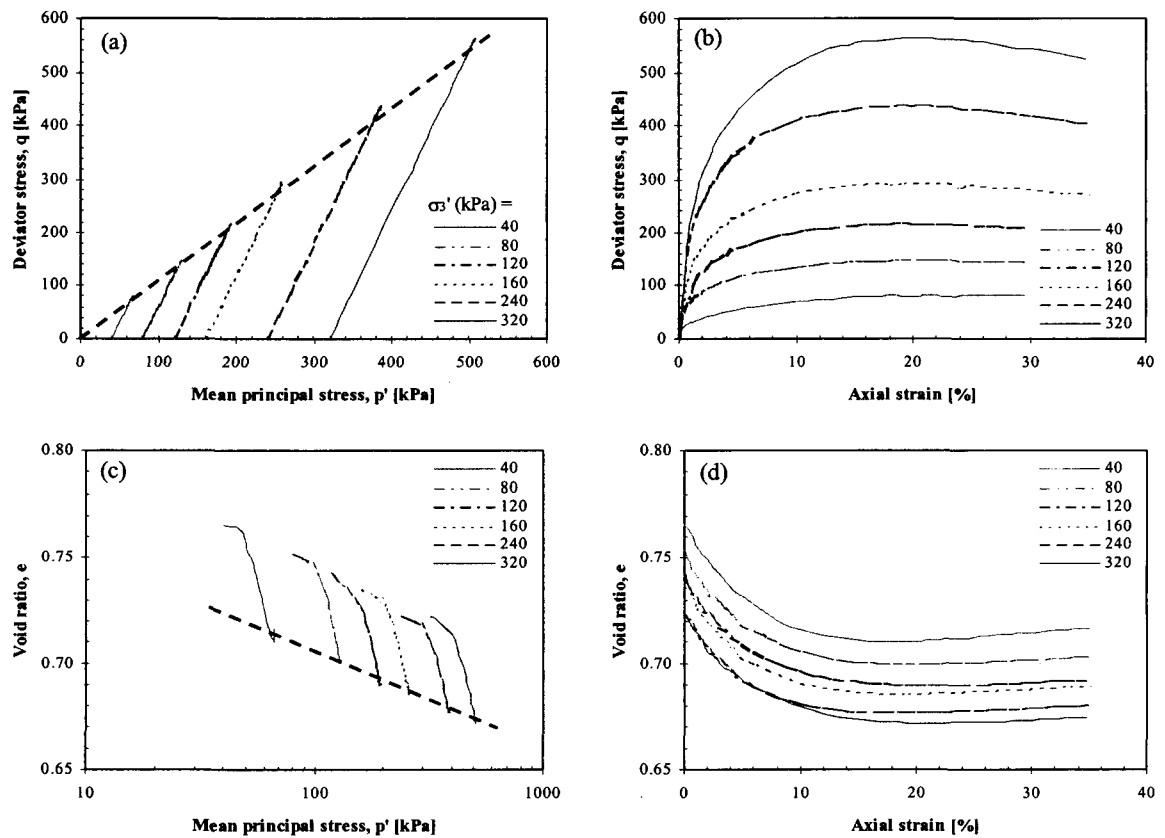


Fig. 6. Drained test results for Ottawa20-30 sand with varying effective confining stresses and similar initial void ratio

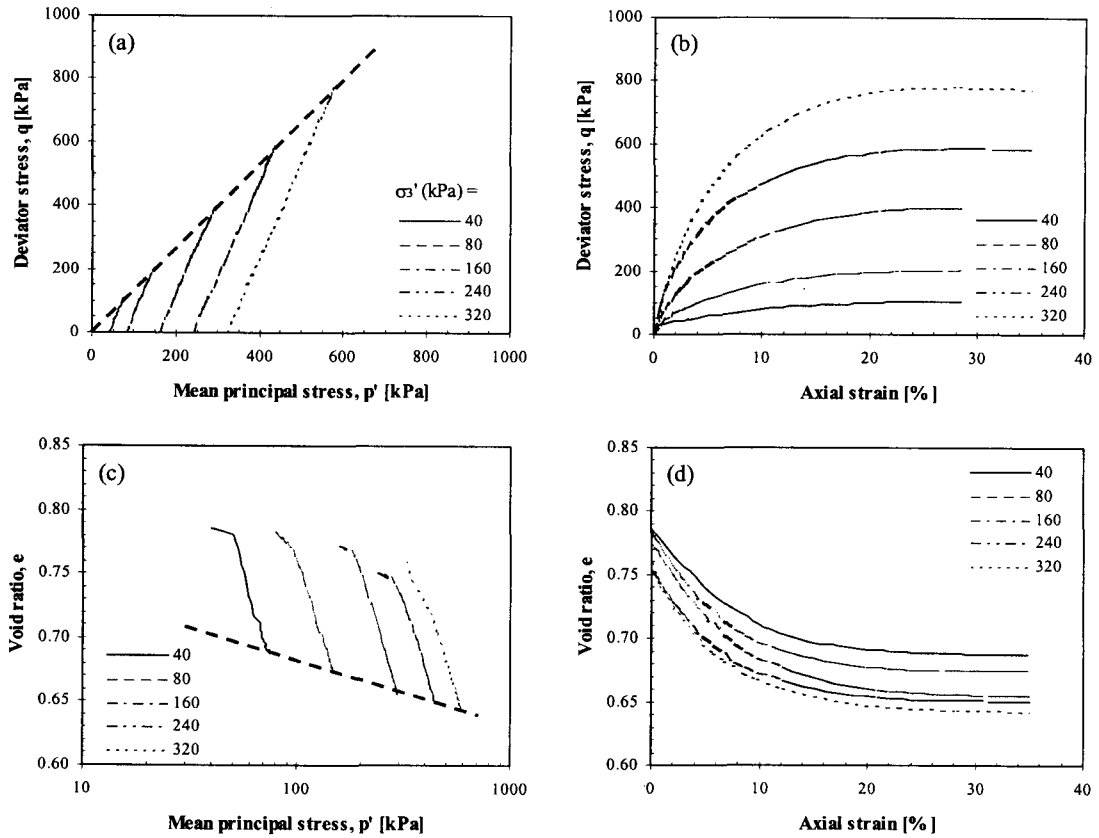


Fig. 7. Drained test results for sandboil sand with varying effective confining stresses and similar initial void ratio

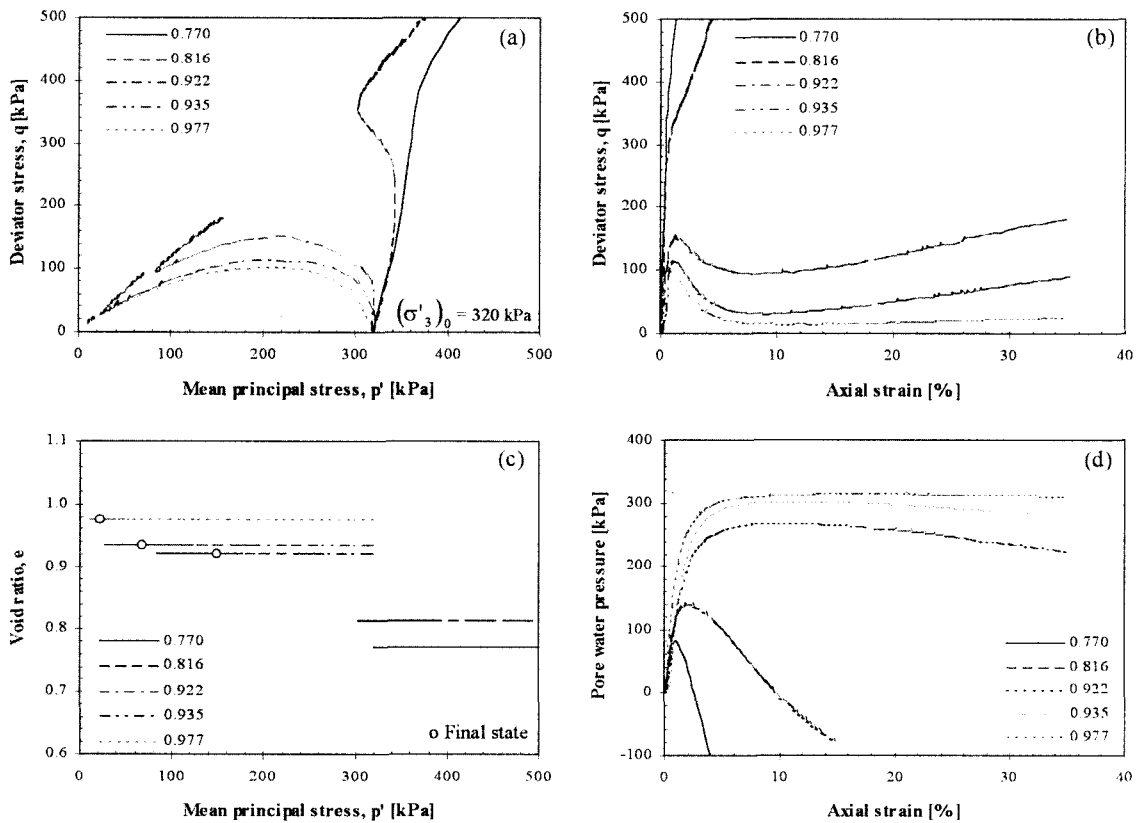


Fig. 8. Undrained test results for blasting sand with different void ratio at the same initial effective confining stress

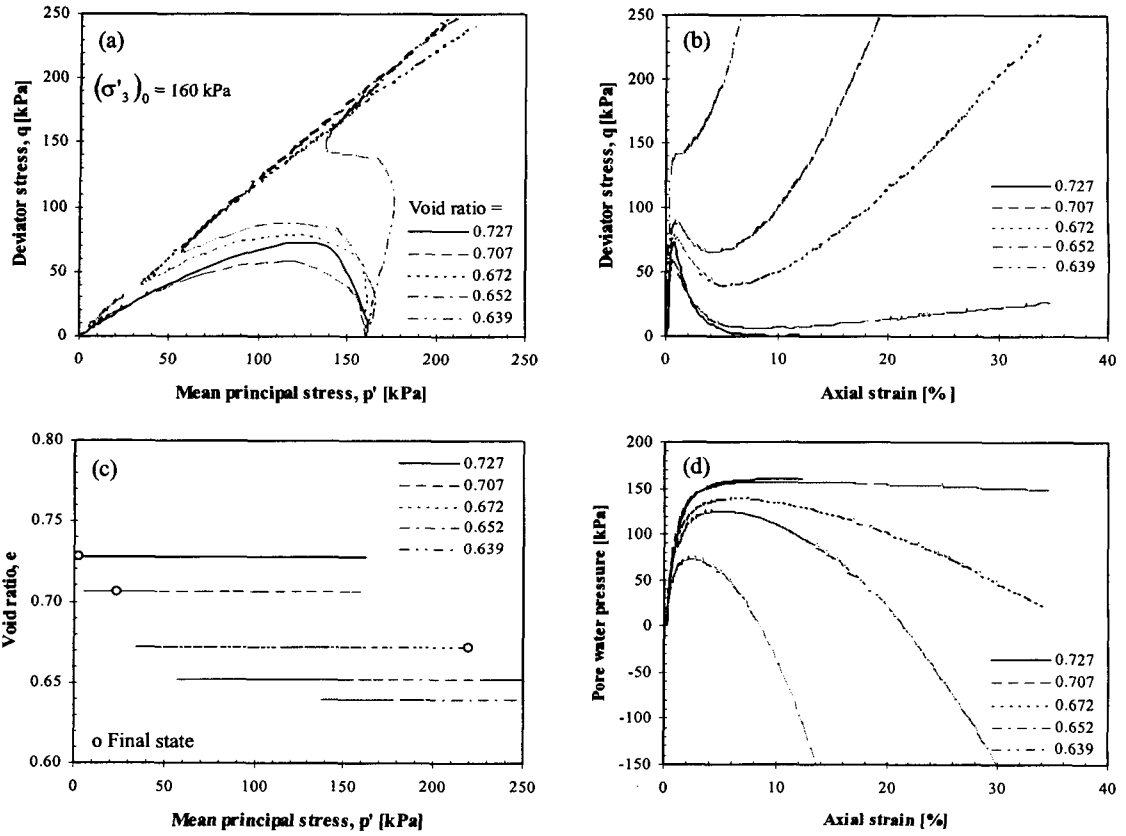


Fig. 9. Undrained test results for Ottawa 20-30 sand with different void ratio at the same initial effective confining stress

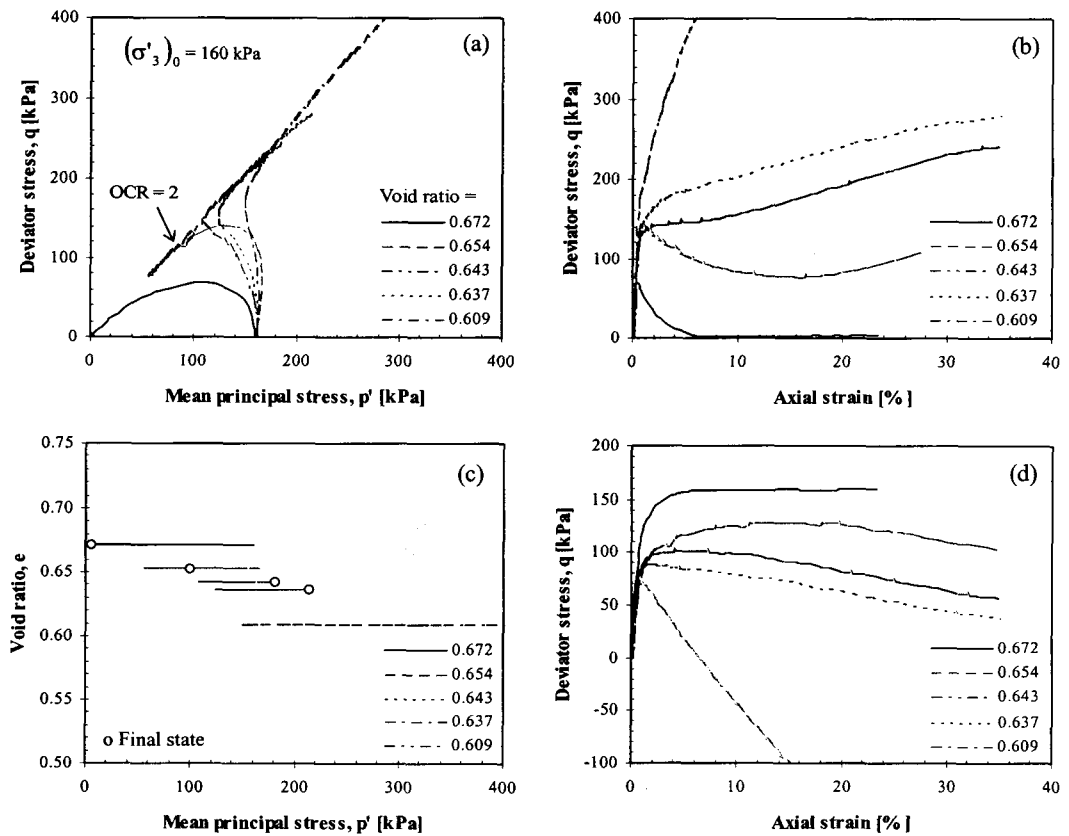


Fig. 10. Undrained test results for sandboil sand with different void ratio at the same initial effective confining stress

3.2 Undrained Test Results

Figures 8, 9 and 10 show undrained test results for the three soils with specimens prepared at different void ratios but confined to the same initial effective confining stress. The stress-strain response is determined by the initial void ratio. Loose/contractive specimens display post-peak behavior and strain localization should be expected. Meanwhile, dense/dilative specimens show the strain-hardening behavior (water cavitation may be reached). It is worth noting that unlike the drained test results, most undrained test results do not reach critical state even at axial strains in excess of 30%. Thus, critical state strength may not be properly determined with undrained tests. One isotropically preloaded specimen

was tested and its results confirm that preloading does not affect the critical state strength (Fig. 10a).

3.3 Comparison Between Drained and Undrained Test Results

Figures 11, 12 and 13 show the comparison between drained and undrained test results for the three sands. There is good agreement between drained and undrained test results on the p' - q space in terms of M , but there is a significant difference on e - $\log p'$ space in terms of Γ and λ . The projection of the critical state line on the e - $\log p'$ space from drained tests renders a higher intercept than from undrained tests. This discrepancy in the critical state line projection on the e - $\log p'$ space is

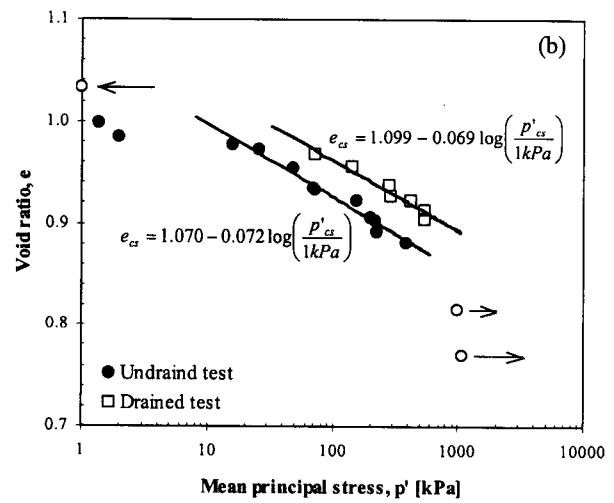
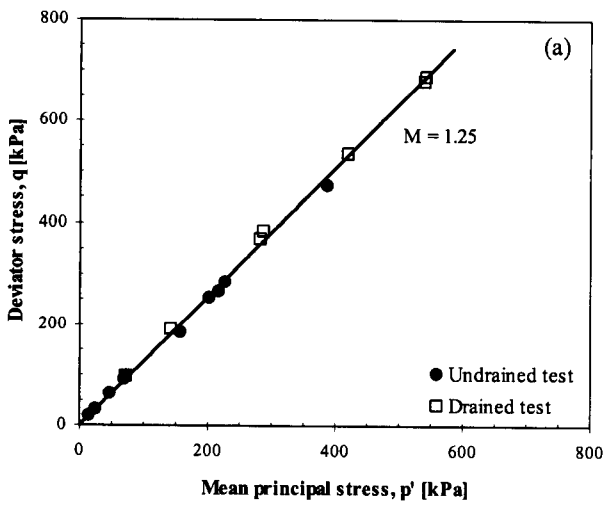


Fig. 11. Comparison between drained and undrained test results for blasting sand

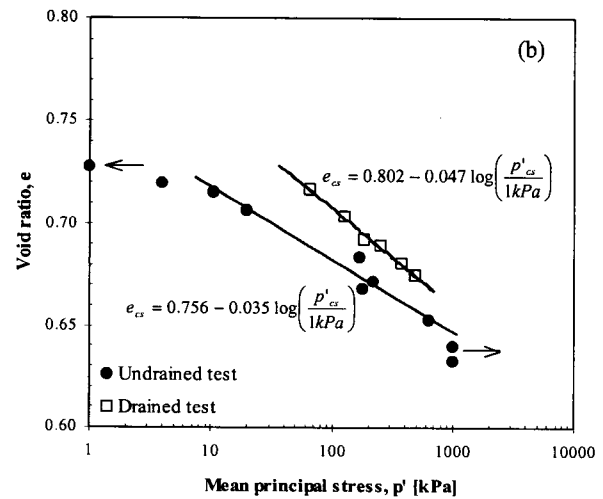
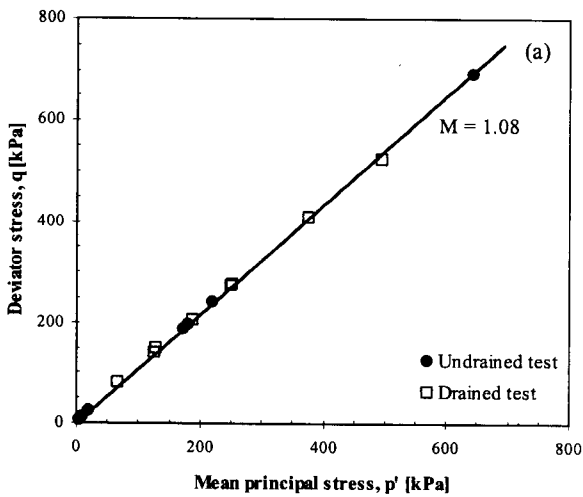


Fig. 12. Comparison between drained and undrained test results for Ottawa 20-30 sand

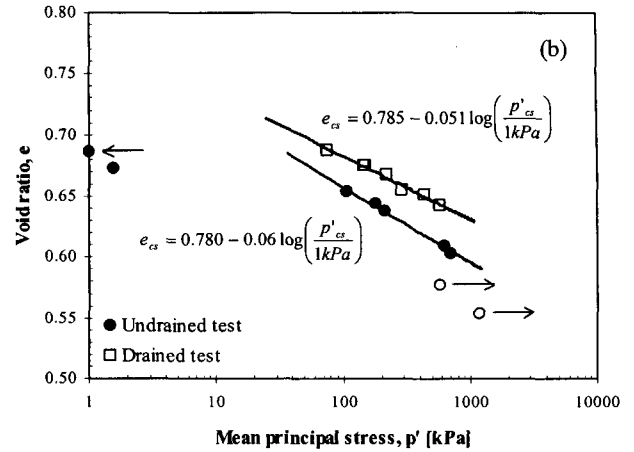
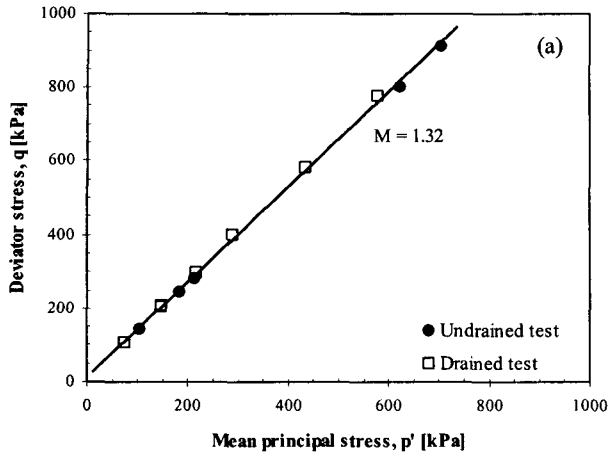


Fig. 13. Comparison between drained and undrained test results for sandboil sand

attributed to insufficient strain level in standard triaxial testing as well as localization in undrained tests. On the other hand, results in Figures 11 (a), 12 (a) and 13 (a) seem to indicate that limitations in strain level and localization do not have an impact on the measured critical state friction angle (p' - q projection).

4. Discussion

4.1 Stress Dilatancy Behavior

As given in the former paper, the energy-based analysis proposed by Taylor (1948) and Bishop (1950; 1954) supports the Mohr-Coulomb criterion. For axisymmetric compression tests (Fedaa, 1982), the stress dilatancy

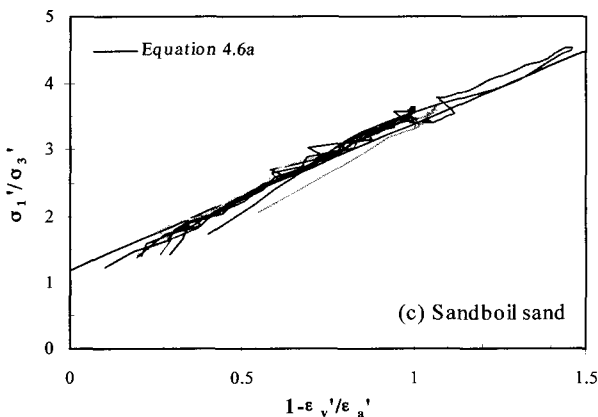
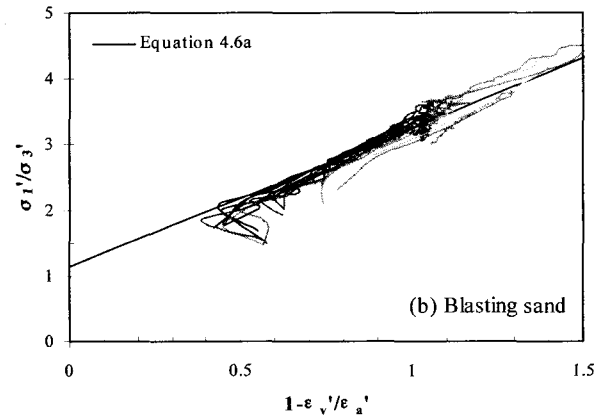
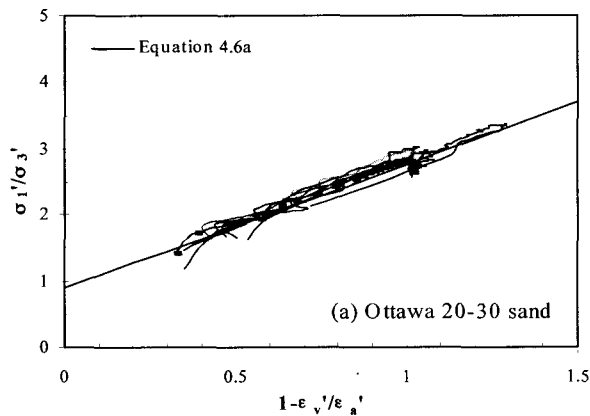


Fig. 14. Stress-dilatancy behavior for three different soils at different confining stresses

Sand	# of tests	Confining stress [kPa]
(a) Ottawa 20-30	9	
(b) Blasting	17	40, 80, 160, 240, 320
(c) Sandboil	10	

equation is:

$$\frac{\sigma'_1}{\sigma'_3} = \frac{1 - \dot{\epsilon}_v / 1 - \dot{\epsilon}_a}{1 - \sin \phi_{cs}} + \frac{\sin \phi_{cs}}{1 - \sin \phi_{cs}}$$

at any stress ratio (1)

Fig. 14 shows the stress dilatancy behavior for the three soils at different confining stresses. The effective stress ratio is directly related to the ratio of increments of strains in terms of critical state friction angle.

4.2 Recommended Test Procedure to Determine CS Parameters

Chu and Lo (1993) suggested the use of dilative specimens subjected to drained loading to failure, followed by undrained shear to measure constant stress at constant volume. However, the soil in the specimen has localized most likely during the first stage.

Verdugo and Ishihara (1996) recommended using the undrained tests (mostly on contractive specimens) to avoid the scatter in drained test results. However, the main reason for the scatter is attributed to strain localization in medium dense and dense specimens subjected to drained tests.

Been et al. (1991) recommended using drained tests on dense specimens or undrained tests on loose specimens to obtain the critical state line. However, both test conditions are prone to strain localization.

Most researchers, who study the flow liquefaction and the instability of landslides, recommend using high confining stresses to promote contractive tendency in undrained triaxial compression testing (Casagrande, 1975; Poulos, 1981; Vaid and Chern, 1985; Alarcon-Guzman et al., 1988; Konrad, 1990; Ishihara, 1993; Lade and Yamamuro, 1996; Riemer and Seed, 1997). However, this procedure is likely to cause post-peak, localization behavior and to hinder the proper assessment of critical state parameters. While localization is expected in the field, laboratory studies must attempt to identify the response of “a point” in the medium, through the homogeneous deformation of the specimen.

Based on results presented in this paper and the study

of localization in Cho (2001), it is suggested that the best method to determine critical state parameters involves testing homogeneous loose specimens subjected to drained shearing. This approach prevents strain localization (or shear banding) observed in the dilative-drained, contractive-undrained and dilative-undrained (cavitation) cases. The critical state points should be selected at the ultimate state after large strains. Thus, this approach renders a unique critical state line for a given soil.

For completeness, the conventional triaxial test has been used for the determination of critical state parameters. However, it is time-consuming and the required set of tests is relatively expensive for common geotechnical tasks. Thus, a simplified test procedure (named simple CS test procedure) is developed by Santamarina and Cho (2001) to determine critical state parameters for sandy soils. On the grounds of economics, effectiveness, and accuracy, the simple CS test procedure appears as a very convenient and reliable alternative approach for the determination of critical state parameters.

4.3 Reference State Parameter

A “softening factor” can be defined following Cornforth (1973)’s density factor. For drained, axial compression triaxial test ($\sigma'_3 = \text{constant}$),

$$\text{softening factor} = \frac{(\sigma'_1 - \sigma'_3)_{\max}}{(\sigma'_1 - \sigma'_3)_{\text{ult}}} - 1 \quad (2)$$

where σ'_1 and σ'_3 are the major and minor principal effective stresses, respectively, “max” is the maximum state, and “ult” is the ultimate critical state. The softening factor approaches 0.0 for specimens with loose, contractive (no post-peak), strain hardening behavior, which experience no localization. The softening factor can be related to the state parameter, which is the difference of initial void ratio and the void ratio at critical state (Been and Jefferies, 1985). Fig. 15 shows the relationship between softening factor and state parameter for the tested sands. As the state parameter decreases, the softening factor increases for all soils. The relationship between the softening factor and the state parameter is

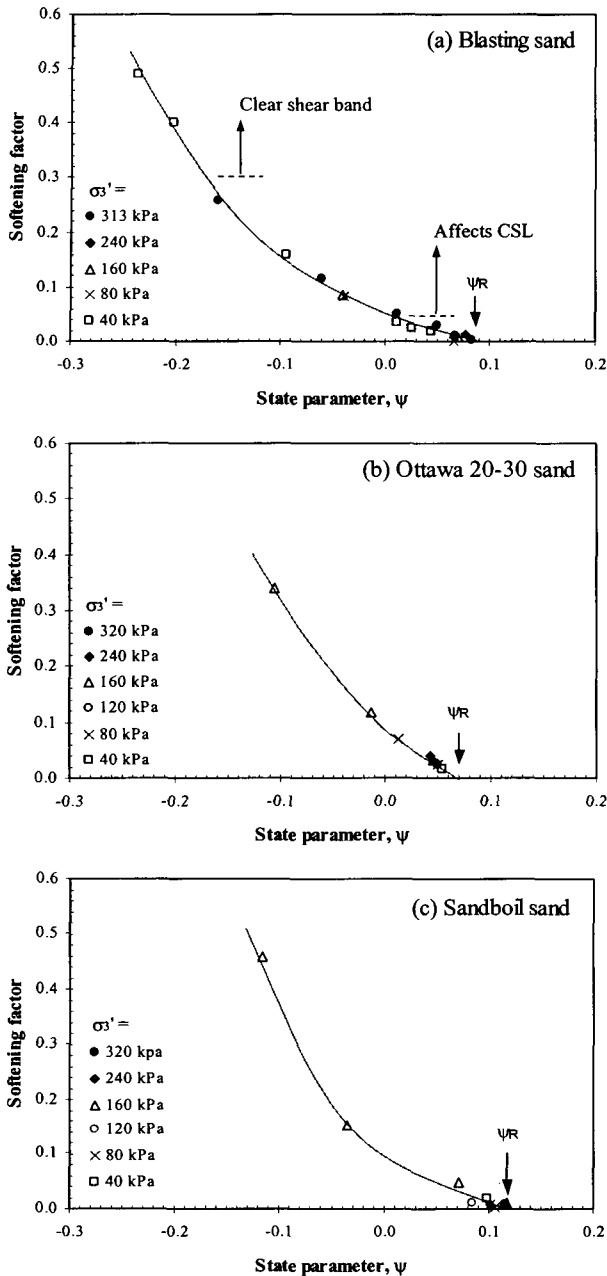


Fig. 15. Relationship between softening factor and state parameter for the tested soils. Notation: Points are from experimental tests and a solid line is a general trend. The reference state parameter Ψ_R is the state parameter where the softening factor is zero.

unique for a soil regardless of the confining stresses. The slope of the trend between the state parameter and the softening factor is inversely related to the slope of critical state line. Two regions can be identified in Fig. 15 (a). Clear shear banding and localization appear when the softening factor exceeds about 0.3. Even low softening factors, however, are associated with shifts in the critical state line (e - $\log p'$ space). The state parameter at which

the softening factor is nil is herein called the reference state parameter Ψ_R . The reference state parameters for blasting, Ottawa 20-30 sand, and sandboil sands are $\Psi_R = 0.085$ ($C_u = 1.94$), $\Psi_R = 0.07$ ($C_u = 1.15$), and $\Psi_R = 0.12$ ($C_u = 2.41$), respectively. It appears that as angularity and the coefficient of uniformity C_u increase, the reference state parameter Ψ_R increases.

These results suggest that in order to avoid dilatancy or localization effects in drained tests, the initial void ratio of the specimen should be greater than the critical state void ratio e_{cs} corresponding to the given state of stress increased by the reference state parameter Ψ_R . Alternatively, a higher confining stress can be applied to cause definite loose contractive condition, for an initial void ratio e_0 . The confining stress should satisfy the following constraint:

$$\sigma'_3 \geq 10^{(\Gamma + \Psi_R - e_0)/\lambda} \cdot 1 \text{ kPa} \quad (3)$$

where the critical state parameters Γ and λ are the intercept (at 1 kPa) and the slope of critical state line on the e - $\log p'$ space, respectively.

According to experimental results at very low effective confining stresses performed on the Space Shuttle by Sture et al. (1998), the dilatancy angle can reach 30 to 31 (note that 35.3 of dilatancy is expected for the dense tetrahedral packing). Considering a critical state friction angle of 30° , the maximum softening factor will be around 9.0, and the state parameter will be negative and close to the interval of $e_{\min} - e_{\max}$. Note that the critical state void ratio at very low confining stress like 1 kPa can be greater than the maximum void ratio (see also Sture et al., 1988). Therefore, even very loose specimen can dilate at sufficiently low confining stresses.

5. Conclusions

The goals of this paper were to identify underlying physical processes and inherent limitations through experimental tests, and to suggest a proper procedure to determine critical state parameters from standard triaxial testing. The main findings are as follows:

- (1) When soil specimens are subjected to drained shearing, the shear stress approaches a similar value regardless of the initial void ratio of specimens. However, globally computed void ratios do not converge to the same value due to strain localization in the dense specimens, which develop shear bands during testing.
- (2) The ultimate state at large strains, at least more than 30% axial strain, should be considered as critical state. Otherwise, the uniqueness of critical state parameters for a given soil will be violated.
- (3) The drainage condition, i.e. undrained or drained condition, little affects the critical state friction angle but does affect the critical state line on the e -log p' space significantly because of insufficient strain attained in standard triaxial tests and strain localization effects in undrained tests.
- (4) The effective stress ratio is directly related to the ratio of increments of strains in terms of critical state friction angle, showing a unique relationship for a given soil.
- (5) The best method to determine critical state parameters in laboratory testing is to use homogeneous loose specimens under drained shear condition. This approach prevents strain localization. Otherwise, reliable critical state parameters may not be obtained from standard triaxial testing.
- (6) The state parameter is related to the proposed softening factor regardless of effective confining stresses. The trend of the softening factor against the state parameter is dependent upon soil type.
- (7) The suggested reference state parameter Ψ_R can be used to design experiments that will avoid any dilatancy and localization effects in drained tests. It is recommended that at a given confining stress, the initial void ratio should be greater than the sum of the reference state parameter and the critical state void ratio.

Acknowledgment

This paper is supported by the Smart Infra-Structure

Technology Center (SISTeC) under the KOSEF Grant ERC 2002.

References

1. Alarcon-Guzman, A., Leonards, G.A., and Chameau, J.L. (1988), "Undrained monotonic and cyclic strength of sand", *Journal of Geotechnical Engineering*, ASCE, Vol.114, No.2, pp.1089-1109.
2. Ambraseys, N.M. (1988), "Engineering seismology", *1st Mallet-Milne Lecture, Journal of Earthquake Engineering and Structural Dynamics*, 17B, pp.1-10.
3. Been, K. and Jefferies, M.G. (1985), "A state parameter for sands", *Géotechnique*, Vol.35, No.2, pp.99-11.
4. Been, K., Jefferies, M.G., and Hachev, J. (1991), "The critical state of sands", *Géotechnique*, Vol.41, No.3, pp.365-381.
5. Bishop, A.W. (1950), "Discussion: Measurement of the shear strength of soils", *Géotechnique*, Vol.2, No.1, pp.113-116.
6. Bishop, A.W. (1954), "Correspondence on shear characteristics of a saturated silt measured in triaxial compression", *Géotechnique*, Vol.4, No.1, pp.43-45.
7. Casagrande, A. (1975), "Liquefaction and cyclic deformation of sands a critical review", *The 5th Panamerican conference on Soil Mechanics and Foundation Engineering*, Vol.5, pp.81-133.
8. Casagrande, A. (1976), "Liquefaction and cyclic mobility of sands: a critical review", *Harvard Soil Mechanics Series 88*, Harvard University, Cambridge, Massachusetts.
9. Castro, G. (1969), *Liquefaction of sands*, Ph.D. thesis, Harvard Soil Mechanics Series, No.81, Harvard University, Cambridge, MA.
10. Chinese building code (1974), *Earthquake-resistant design code for industrial and civil buildings*, A.C.S. Chang (trans.), TJ11-74, State Capital Construction Commission Peoples' Republic of China, China Building Publishing House, Peking, China.
11. Chu, J. and Lo, S.C.R. (1993), "On the measurement of critical state parameters of dense granular soils", *Geotechnical Testing Journal*, GTJODJ, Vol.16, No.1, pp.27-35.
12. Cho, G.C. (2001), *Unsaturated Soil Stiffness and Post-Liquefaction Shear Strength*, Ph.D. Thesis, Georgia Institute of Technology, Atlanta, USA, p.288.
13. Cornforth, D.H. (1973), "Prediction of drained strength of sands from relative density measurements", *Evaluation of relative density and its role in geotechnical projects involving cohesionless soils*, ASTM STP 523, American Society for Testing and Materials, Philadelphia, pp.281-30.
14. Desrues, J., Chambon, R., Mokni, M., and Mazerolle, F. (1996), "Void ratio evolution inside shear bands in triaxial sand specimens studied by computed tomography", *Géotechnique*, Vol.46, No.3, pp.529-54.
15. Dobry, R., Ladd, R.S., Yokel, F.Y., Chung, R.M., and Powell, F. (1982), *Prediction of pore water pressure buildup and liquefaction of sands during earthquakes by the cyclic strain method*, National Bureau of Standards, NBS Building Science Series 138, p.150.
16. Feda, J. (1982), *Mechanics of particulate materials*, Developments in Geotechnical Engineering No.30, Elsevier.
17. Finn, W.D.L., Ledbetter, R.H., and Wu, G. (1994), "Liquefaction in silty soils: Design and analysis", *Ground Failures under Seismic Conditions, Geotechnical Special Publication 44*, ASCE, New York,

- pp.51-76.
18. Hird, C.C., and Hassona, F.A.K. (1990), "Some factors affecting the liquefaction and flow of saturated sands in laboratory tests", *Engineering Geology*, Vol.28, pp.149-17.
 19. Ishihara, K. (1993), "The Rankine Lecture: Liquefaction and flow failure during earthquakes", *Géotechnique*, Vol.43, No.3, pp.351-415.
 20. Konrad, J.M. (1990), "Minimum undrained strength versus steady-state strength of sands", *Journal of Geotechnical Engineering*, Vol. 116, No.6, pp.948-963.
 21. Kramer, S.L. (1996), *Geotechnical Earthquake Engineering*, Prentice-Hall, Inc., page 65.
 22. Lade, P.V., and Yamamuro, J.A. (1996), "Undrained sand behavior in axisymmetric tests at high pressures", *Journal of Geotechnical Engineering*, Vol.122, No.2, pp.120-129.
 23. Liao, S.S.C., Veneziano, D., and Whitman, R.V. (1988), "Regression models for evaluating liquefaction probability", *Journal of Geotechnical Engineering*, ASCE, Vol.114, No.4, pp.389-411.
 24. Park, J.Y. (2000), *A Critical Assessment of Moist Tamping and Its Effect on the Initial and Evolving Structure of Dilatant Triaxial Specimens*, Ph.D. Thesis, Georgia Institute of Technology, Atlanta, USA, p.384.
 25. Poulos, S.J. (1981), "The steady state of deformation", *Journal of Geotechnical Engineering*, Vol.107, No.GT5, pp.553-562.
 26. Poulos, S.J., Castro, G., and France, J.W. (1985), "Liquefaction evaluation procedure", *Journal of Geotechnical Engineering*, Vol.111, No.6, June, pp.772-792.
 27. Riemer, M.F. and Seed, R.B. (1997), "Factors affecting apparent position of steady-state line", *Journal of Geotechnical and Geoenvironmental Engineering*, Vol.123, No.3, pp.281-288.
 28. Robertson, P.K. and Campanella, R.G. (1985), "Liquefaction potential of sands using the CPT", *Journal of Geotechnical Engineering*, Vol.111, No.GT3, pp.384-403.
 29. Santamarina, J.C., and Cho, G.C. (2001), "Determination of critical state parameters in sandy soils - Simple procedure", *Geotechnical Testing Journal*, GTJODJ, Vol.24, No.2, June, pp.185-192.
 30. Seed, H.B. (1979), "Soil liquefaction and cyclic mobility evaluation for level ground during earthquakes", *Journal of the Geotechnical Engineering Division*, ASCE, Vol.105, No.GT2, pp.201-255.
 31. Seed, H.B. and Idriss, I.M. (1971), "Simplified procedure for evaluating soil liquefaction potential", *Journal of the Soil Mechanics and Foundation Division*, ASCE, Vol.97, No.SM9, pp.1249-1273.
 32. Seed, H.B., Idriss, I.M., and Arango, I. (1983), "Evaluation of liquefaction potential using field performance data", *Journal of Geotechnical Engineering*, Vol.109, No.GT3, pp.458-482.
 33. Sture, S., Costes, N.C., Batiste, S., Lankton, M.R., AlShibli, K.A., Jeremic, B., Swanson, R.A., and Frank, M. (1998), "Mechanics of granular materials at low effective stresses", *Journal of Aerospace Engineering*, Vol.11, No.3, pp.67-72.
 34. Taylor, D.W. (1948), *Fundamentals of Soil Mechanics*, John Wiley & Sons, Inc., p.770.
 35. Vaid, Y.P. and Chern, J.C. (1985), "Effect of static shear on resistance to liquefaction", Discussion, *Soils and Foundations*, Japanese Society of Soil Mechanics and Foundation Engineering, Vol.25, No.3, pp.54-156.
 36. Verdugo, R. and Ishihara, K. (1996), "The steady state of sandy soils", *Soils and Foundations*, Vol.36, No.2, pp.81-91.
 37. Wang, W. (1979), *Some findings in soil liquefaction*, Water Conservancy and Hydroelectric Power Scientific Research Institute, Beijing, China.
 38. Wood, D.M. (1990), *Soil behavior and critical state soil mechanics*, Cambridge University Press, Cambridge, Mass.
 39. Youd, T.L. (1991), "Mapping of earthquake-induced liquefaction for seismic zonation", *Proceedings of 4th International Conference on Seismic Zonation*, Earthquake Engineering Research Institute, Stanford University, Vol.1, pp.111-147.
 40. Youd, T.L., and Hoose, S.N. (1977), "Liquefaction susceptibility and geologic setting", *Proceedings of 6th World Conference on Earthquake Engineering*, New Delhi, Vol.3, pp.2189-2194.
 41. Youd, T.L., and Idriss, I.M. (1997), *Proceedings of NCEER Workshop on Evaluation of Liquefaction Resistance of Soils*, Technical Report NCEER-97-0022, p.276.
 42. Zhou, S. (1980), "Evaluation of the liquefaction of sand by static cone penetration test", *Proceedings of the 7th World Conference on Earthquake Engineering*, held at Istanbul, Turkey, Vol.3, pp.156-162.

(received on Jul. 30, 2002, accepted on Dec. 23, 2002)